Supporting Information: A DNA-based Optical Sensor for Forces in Cytoskeletal Networks

Christina Jayachandran,[†,‡,▽] Arindam Ghosh,[†,¶,▽] Meenakshi Prabhune,[†] Jonathan Bath,[§,‖] Andrew Turberfield,[§,‖] Lara Hauke ,[†,⊥] Jörg Enderlein,[†,#] Florian Rehfeldt,[*,†,@] and Christoph F. Schmidt[*,†,△]

†*Third Institute of Physics—Biophysics, Georg August University, Friedrich-Hund-Platz 1, 37077 Göttingen, Germany*

‡*Department of Pharmacy - Center for Drug Research, Pharmaceutical Biology, Ludwig-Maximilians University, Munich, Bavaria, 81377, Germany*

¶*Department of Biotechnology and Biophysics, Biocenter, University of Würzburg, Am Hubland, 97074 Würzburg, Germany.*

§*Department of Physics, Clarendon Laboratory, University of Oxford, Oxford, OX1 3PU, UK*

‖*The Kavli Institute for Nanoscience Discovery, University of Oxford, Oxford, OX1 3QU, UK*

⊥*Institute of Pharmacology and Toxicology, University Medical Center, Robert-Koch-Str. 40, 37075 Göttingen, Germany*

#*Cluster of Excellence "Multiscale Bioimaging: from Molecular Machines to Networks of Excitable Cells" (MBExC), Georg August University, Göttingen, Germany*

@*Experimental Physics I, University of Bayreuth, Universitätsstr. 30, 95440 Bayreuth, Germany*

△*Department of Physics and Soft Matter Center, Duke University, Durham, NC 27708, United States.*

▽*C.J. and A.G. contributed equally to this work*

E-mail: *florian.rehfeldt@uni-bayreuth.de; *cfschmidt@phy.duke.edu

Fluorescence lifetime data evaluation

Fluorescence lifetime data were analyzed using a custom-written MATLAB routine. Data evaluation for sensors in the aqueous buffer as presented in Figure 2b of the main text was done as follows: first, TCSPC histograms were computed from the recorded photons. A mono-exponential decay function was fitted to the tail of the histogram (0.5 ns after the maximum) for donor only and opened sensors using a maximum likelihood procedure. The fitting function was:

$$I(t) = \frac{A}{\tau} e^{\frac{-t}{\tau}} + b \tag{1}$$

where τ is the fluorescence lifetime, *A* the amplitude, and *b* the background. The negative log-likelihood was minimized using a Nelder-Mead simplex algorithm. Initial parameters for the optimization were obtained by choosing the parameter set that minimizes the least-squares error from a collection of exponential functions. For closed sensors, TCSPC histogram was tail-fitted (0.2 ns after the maximum) similarly but with a bi-exponential decay function. Figure 2b shows representative TCSPC histograms and their fits for closed, open, and donor only sensors. For estimating the mean lifetime value and standard deviation, TCSPC histograms from three independent experiments for each type of sensor was considered.

Data evaluation for FLIM imaging of *in vitro* actin networks was done as follows: A bi-exponential decay function was fitted to the tail of TCSPC histograms (0.2 ns after maximum) as accumulated from each virtual pixel of the single-photon detector in case of closed sensors. Fluorescence lifetime histogram as presented in Figure 3d illustrate the short and long lifetime components obtained from the fit and their occurrence in each pixel. We also calculated the intensity-weighted average fluorescence lifetime of these two components. Figure 3d represent lifetime values from a representative *z* stack of a

measurements. Lifetime fitting was done in a similar way for all *z* slices in two independent experiments. TCSPC data from donor only sensors inside actin networks were fitted with monoexponential decay function. For a single-shot FLIM imaging in HeLa cells as shown in Figure S8, we fitted each pixel with a bi-exponential function and the intensity-weighted average values are shown as false color in Figures S8b and S8c.

Unzipping force of DNA force sensors

We estimated the characteristic force $F_{1/2}$ for the opening of the DNA hairpin loop of our sensors based on published results, balancing the work done by the external force with the free energy change associated with the hairpin unfolding process.[1] $F_{1/2}$ is the force at which 50 % of the sensors are expected to be extended and is calculated as:

$$F_{1/2} = \frac{\Delta G_{fold} + \Delta G_{stretch}}{\Delta x}. \tag{2}$$

The free energy of unfolding ΔG_{fold} , which is the hybrization free energy of the double-stranded stem, is calculated using the IDT oligoanalyzer tool 3.1 for the chosen hairpin strand sequence. $\Delta G_{stretch}$ is the elastic free energy of the fully unfolded and stretched hairpin loop of length x at force $F_{1/2}$, calculated from the worm-like chain model as:[2]

$$\Delta G_{stretch} = \frac{k_B T}{L_p} \frac{L_c}{4(1-\frac{x}{L_c})} \left[3(\frac{x}{L_c})^2 - 2(\frac{x}{L_c})^3 \right], \tag{3}$$

where k_B is the Boltzmann constant, T is the temperature (23° for *in vitro* experiments and 37° for *in cellulo* experiments). L_p is the persistence length of ssDNA calculated for the respective ionic conditions of *in vitro* actin networks and *in cellulo* (Table S9). Only the dominant divalent ions (Mg^{2+}) were considered for the calculation, following published

work:[3]

$$L_p = L_p^0 + L_p^{el} \tag{4}$$

where L_p^0 is the intrinsic persistence length which is 0.7 nm.[3] L_p^{el} is the electrostatic contribution to the persistence length, proportional to the inverse of the square root of ion concentration in solution.[4–8] For our samples, L_p^{el} was calculated as the inverse of the square root of the divalent salt concentration (see Table S9). L_c is the contour length of the DNA hairpin strand. Since L_c values in Na^+ (0.69 nm) and Mg^{2+}(0.7 nm) are almost identical,[3] a contour length of 0.7 nm was used to calculate $F_{1/2}$ *in vitro* and *in cellulo*. For our hairpin of 32 bases, L_c = 22.4 nm and the ssDNA length x at force $F_{1/2}$ is taken as:[2]

$$x = 0.44\ nm \times (n-1), \tag{5}$$

with n representing the number of bases in the hairpin (32 bases). Finally, $F_{1/2}$ is obtained from Eq. 2 by estimating the displacement of the attachment points to the hairpin loop during the opening process as:

$$\Delta x = 0.44\ nm \times (n-1) - 2\ nm. \tag{6}$$

A distance of 2 nm is subtracted for the initial separation between the hairpin termini that corresponds to the diameter of the hairpin stem duplex, i.e. the effective helix width as described by Zhang *et al.*[1] Free intracellular Mg^{2+} concentration is $\sim$ 1 mM,[9,10] which was used for the calculation (Table S7 & S8). The estimated unfolding force $F_{1/2}$ of our sensors *in vitro* is $\sim$ 12 pN and *in cellulo* is $\sim$ 6 pN.

Table S1: DNA oligos sequence

strands	Oligo sequence
F	5'Alexa 488N / CGC TGC GTG CTT TCA GGG CG / Thiol MC3-D 3'
Q	5'Thiol MC6-D / CGC AAG CCG CGT GCC CGC GC / Iowa black FQ 3'
Q^-	5'Thiol MC6-D / CGC AAG CCG CGT GCC CGC GC 3'
H	5'CGC CCT GAA AGC ACG CAG CGG CGA ACC GGA GAG TGT TAG AGA CAC GGT TCG CGC GCG GGC ACG CGG CTT GCG 3'
C	5' TGT CTC TAA CAC TCT CCG GTT CGC 3'

Table S2: Buffer compositions

Buffer types	Composition
DNA hybridization	50 mM NaCl, 10 mM $MgCl_2$, 1x PBS
Actin buffer	1M KCl, 0.1 M imidazole pH 7.4, 10 mM ATP, 20 mM $MgCl_2$

Table S3: DNA sensor crosslinking concentration

Network	R	Sensor concentration [µM]
Actin[a]	0	0
Actin[a]+DNA sensor	0.005	0.12
	0.01	0.24
	0.02	0.48
	0.1	2.4
	0.2	4.7

[a] A fixed actin concentration of 23.81 µM was always used

Table S4: Fluorescence lifetime values (in ns) and their relative fit amplitudes

Closed sensor (µM)	τ (ns) DNA buffer	τ (ns) Actin buffer
F:H:Q (2:2:2)	0.62 $\pm$ 0.04 [0.25]	0.80 $\pm$ 0.08 [0.22]
	3.70 $\pm$ 0.07 [0.75]	3.58 $\pm$ 0.07 [0.78]
F:H:Q (1:2:2)	0.53 $\pm$ 0.04 [0.36]	0.59 $\pm$ 0.02 [0.25]
	3.70 $\pm$ 0.06 [0.64]	3.58 $\pm$ 0.07 [0.75]
F:H:Q (0.5:2:2)	0.53 $\pm$ 0.08 [0.38]	0.59 $\pm$ 0.04 [0.29]
	3.70 $\pm$ 0.07 [0.62]	3.58 $\pm$ 0.05 [0.71]
F:H:Q (0.25:2:2)	0.51 $\pm$ 0.08 [0.43]	0.61 $\pm$ 0.05 [0.29]
	3.70 $\pm$ 0.08 [0.57]	3.58 $\pm$ 0.05 [0.71]

Table S5: Actin-sensor network R = 0.1 fluorescence lifetime values (in ns) and their relative fit amplitudes

Network z-height (µm)	τ_1 **(ns) Closed sensor**	τ_2 **(ns) Closed sensor**	τ **(ns) Opened sensor**
0	0.94 ± 0.06 [0.43]	3.52 ± 0.06 [0.57]	3.87 ± 0.05
1	0.98 ± 0.04 [0.40]	3.52 ± 0.07 [0.60]	3.85 ± 0.07
2	0.94 ± 0.07 [0.37]	3.35 ± 0.08 [0.63]	3.89 ± 0.06
3	0.92 ± 0.06 [0.35]	3.27 ± 0.05 [0.65]	3.89 ± 0.08
4	0.93 ± 0.05 [0.35]	3.20 ± 0.06 [0.65]	3.88 ± 0.04
5	0.90 ± 0.08 [0.33]	3.34 ± 0.06 [0.67]	3.89 ± 0.07

Table S6: Actin-donor only control network R = 0.1 fluorescence lifetime values (in ns) and their relative fit amplitudes

Network z-height (µm)	τ_1 **(ns) Donor only control (closed)**	τ_2 **(ns) Donor only control (open)**
0	3.28 ± 0.05	3.72 ± 0.07
1	3.40 ± 0.07	3.90 ± 0.04
2	3.48 ± 0.06	3.94 ± 0.06
3	3.53 ± 0.08	3.95 ± 0.05
4	3.58 ± 0.04	3.95 ± 0.05
5	3.59 ± 0.07	3.95 ± 0.07

Table S7: $F_{1/2}$ calculation for sensor (stem = 16 bases (8 bp) & loop = 16 bases)

	$\Delta\, G_{fold}$ [kJ/mol]	$\Delta\, G_{stretch}$ [kJ/mol]	Δ **x** [nm]	$\mathbf{F}_{1/2}$ [pN]
in vitro	51.54	30.42	11.64	12
in cellulo	27.73	14.34	11.64	6

[b]Sequence used in calculation of $\Delta\, G_{fold}$ is GCGAACCGGAGAGTGTTAGAGACACGGTTCGC

Table S8: Experimental conditions used for $\Delta\, G_{fold}$ calculation

Experiment	**Salt Concentrations**	**T**	**Sensor**
in vitro actin	200 mM Mg^{2+}	25°C	2.4 µM
in cellulo actin	10 mM Na^{+}, 1 mM Mg^{2+}	37°C	0.05 µM

Table S9: L_p & L_c dependence on ionic conditions

Experiment	**Salt Concentrations**	L_p	L_c
in vitro actin	200 mM $MgCl^{2+}$	0.77 nm	0.7 nm
in cellulo actin	1 mM Mg^{2+}	1.7 nm	0.7 nm

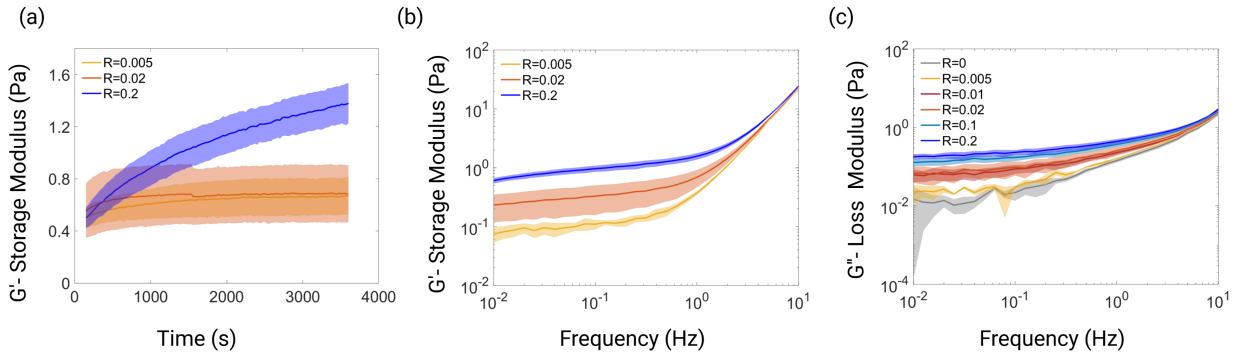

Figure S1: Gelation kinetics and frequency response of actin, actin-DNA sensors networks at different sensor concentrations. **(a):** Gelation kinetics for sensor concentrations (R = 0.005, 0.02, 0.2) to show the evidence of a crosslinked network. **(b),(c):** The frequency response of these networks shows weak power-law behavior in the reliable range of the measurement (<1Hz). Solid lines represent mean values and the shaded area the standard error of mean.

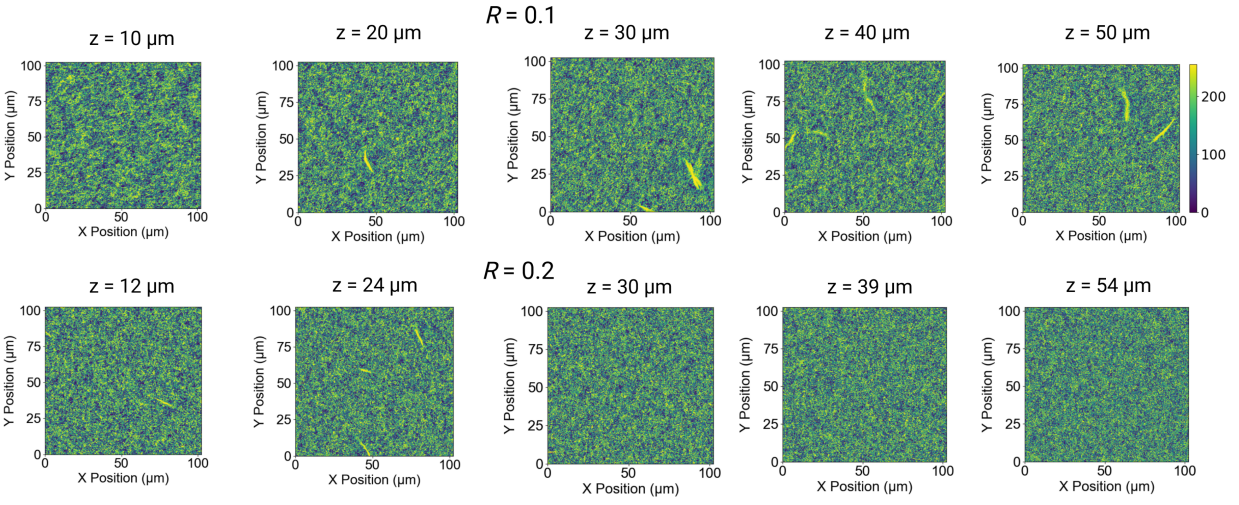

Figure S2: Morphology of R = 0.1 & R = 0.2 actin-DNA sensor networks at varying z-positions in the network. A confocal xyz scan was performed for actin-sensor networks at higher sensor concentrations (R = 0.1, 0.2). Bundling of actin filaments by DNA-sensor was observed mostly in the middle of the network. They were not present at the boundary surfaces of the coverslip and the microscopic slide. Actin is labeled for fluorescence with Atto 647N Phalloidin. Colorbar indicates the brightness of images.

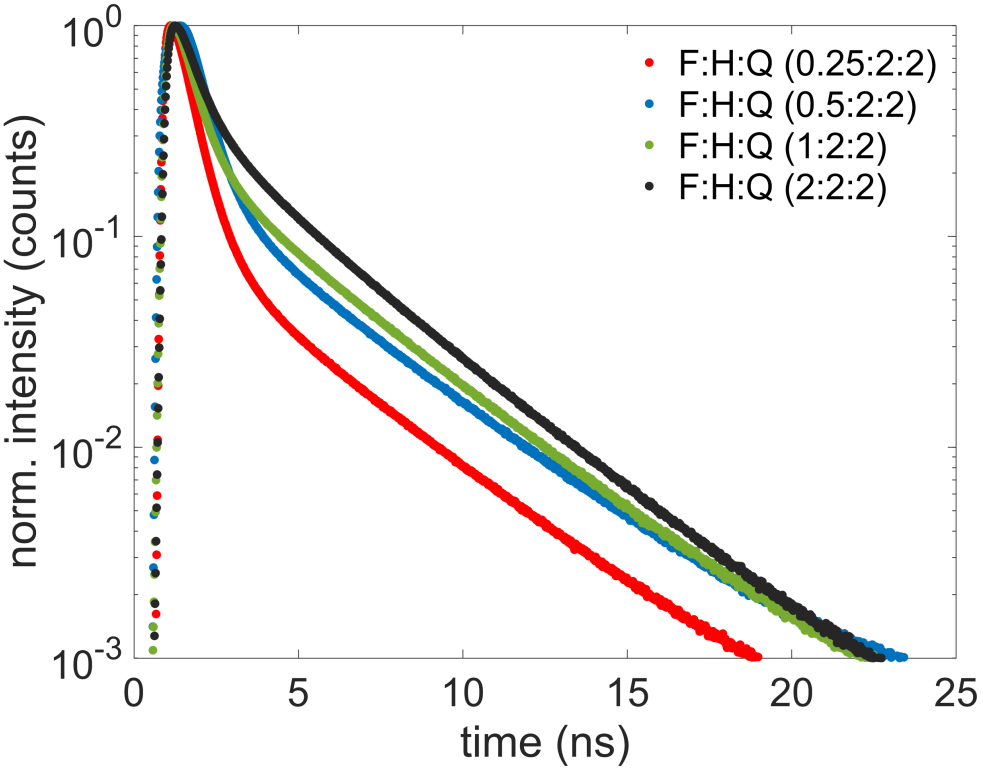

Figure S3: Representative TCSPC decays of closed sensors at various molar ratios in DNA hybridization buffer. Ratios tested are F:H:Q - 0.25:2:2, 0.5:2:2, 1:2:2, and 2:2:2 µM. Legend: Stoichiometric ratio represented in µM

Extended data and figures

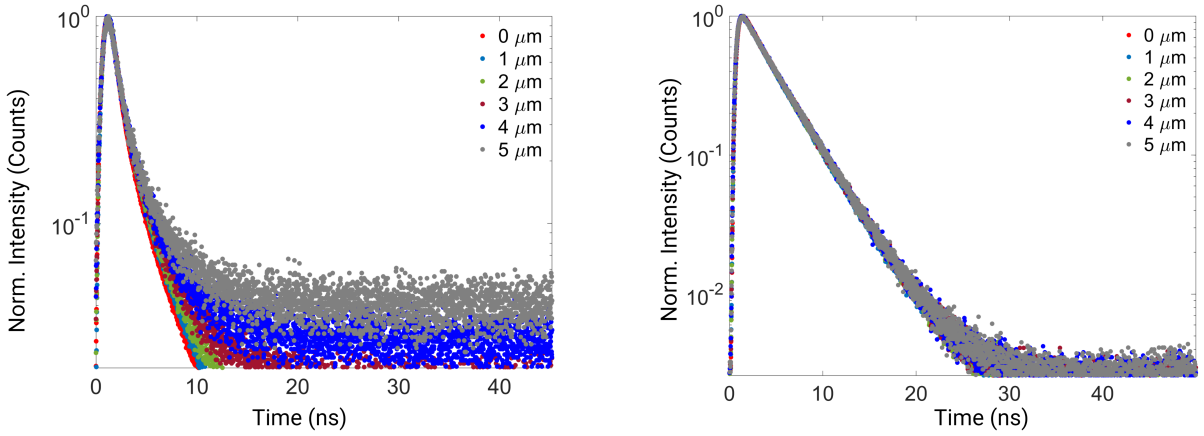

Figure S4: Representative TCSPC decays from each *z* planes at 0, 1, 2, 3, 4, and 5 μm for actin networks crosslinked with closed (left) and donor-only control (right) R = 0.1.

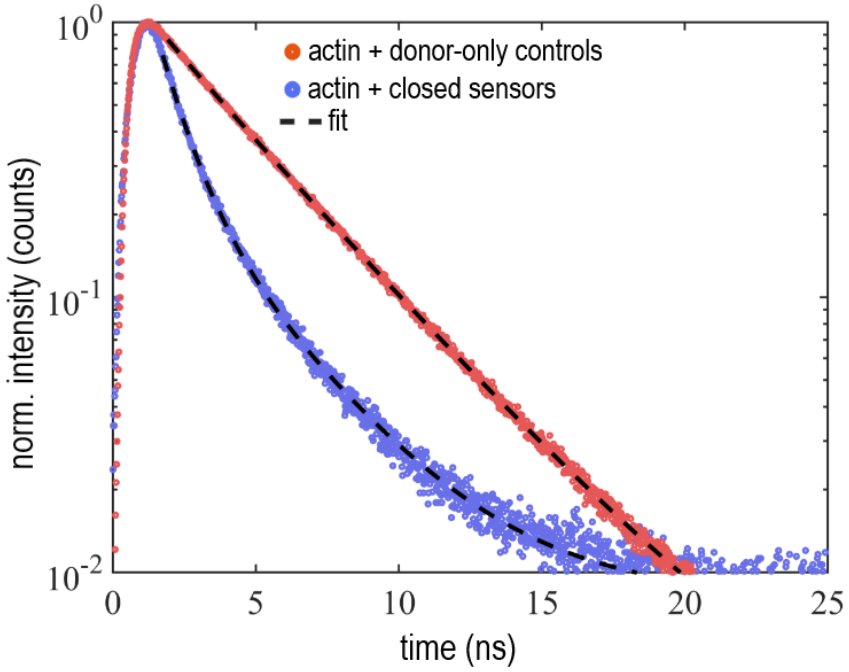

Figure S5: Representative TCSPC decay histograms from z slice 3 µm of closed and donor-only sensors crosslinked to actin networks. Histograms of fitted fluorescence lifetime values are presented in Figure 3D of the main text.

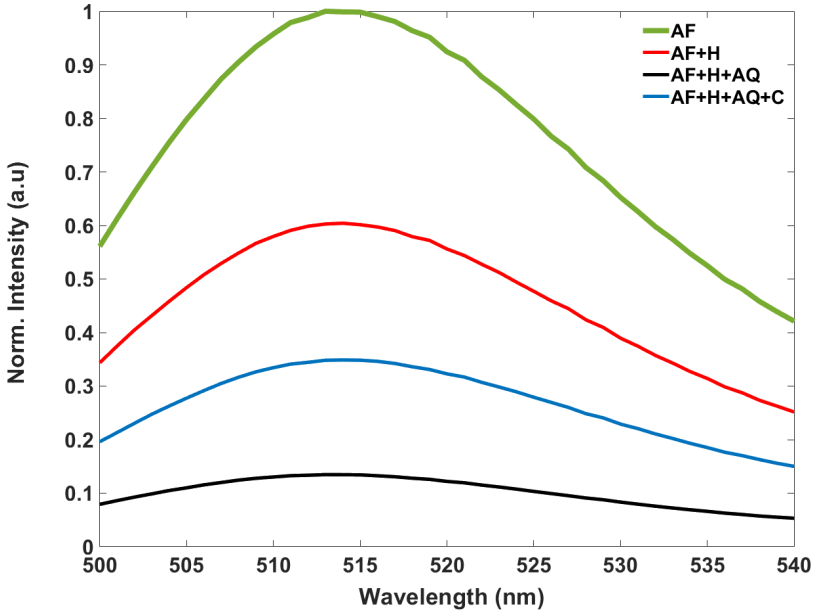

Figure S6: Sequential addition of different strands of sensors while attached to actin for a network of R = 0.1. Emission spectra of DNA sensors crosslinked to actin filaments. AF represents actin attached to the F strand of the sensor which was added in the cuvette first. Next H strands were added to the AF mixture, which is represented as AF+H. The reduction in fluorescence intensity is due to guanosines quenching the alexa488. AQ is actin crosslinked to the Q strand of the sensor, which upon addition to AF+H mixture strongly quenches showing the sensor proof of principle while crosslinked to actin. AF+H+AQ denotes actin attached to F strands+ H strands + Q strands. Lastly upon addition of C (complementary) strand opens the quenched sensors in the actin network with a mild increase in fluorescence. Actin attached to F strand (AF) and AQ were separately polymerized in individual tubes. They were then mixed together in a emission spectral measuremnts by sequential addition of each of sensor strands. Actin concentration in AF and AQ each: 0.5 mg/ml (11.9 µM). 0.5:1:1(F:H:Q) stoichiometry was used.

Introduction of sensors in living cells

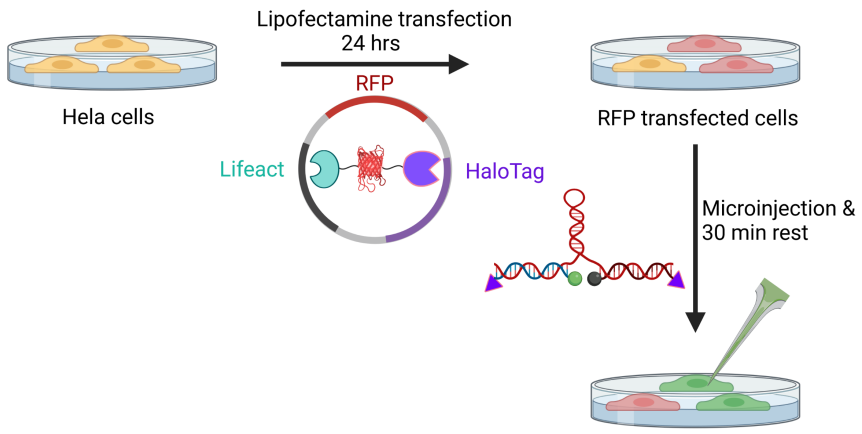

Figure S7: A schematic representation of the transfection protocol of DNA sensors. DNA sensors were transfected into Hela cells in 2 steps. The lifeact-RFP-HaloTag® plasmid was transfected into Hela cells with lipofectamine 3000. 48 h later, a 50 nM solution of DNA sensors that were first modified, were assembled *in vitro* and microinjected near the nucleus. (Scheme is not drawn to scale.)

Preparation of lifeact-RFP-HaloTag® as a protein construct and plasmid

The lifeact-RFP-HaloTag® is genetically fused, expressed as a protein and as a plasmid for employing in *in vitro* actin-DNA sensor networks and in *in cellulo*. Protein expression was performed as follows. BL21 cells were transformed with the plasmid pET28a containing the three fused genes lifeact-RFP-Halotag-His6. They were grown in LB medium containing kanamycin until they reached an optical density (0D) of 0.4-0.5 at 37 °C. The shaker temperature was reduced to 22 °C and induced with 0.1 mM IPTG. Protein expression was carried out overnight at 22 °C. The solution was centrifuged at 4600 xg for 20 min at 4 °C. The pellet was either stored at -80 °C for later use or resuspend in 20 ml lysis buffer per tube, frozen in liquid nitrogen and stored at -80 °C. Protein purification was performed in a NiNTA column (Machery and Nagel Protino NiNTA Agarose (LOT: 1411/002)) according to manufacturer's protocols. The protein concentration was then determined using Bradford assay. For *in cellulo* experiments, the plasmid containing lifeact-RFP-HaloTag® was prepared according to standard procedures except for the

following changes. The lifeact-RFP-HaloTag® was cloned in the pFC14A HaloTag® CMV Flexi® Vector (Cat No #G9651, Promega, Germany) and transformed in DH5α E.coli in a LB medium containing ampicillin as the antiobiotic.

Introduction of sensors into living cells was performed in a two-step procedure (see Figure S7). HeLa cells (ACC 173, Leibniz Institute DMSZ, Braunschweig, Germany) were cultivated to confluency in T75 flasks and passaged as follows. They were rinsed with 10 ml of PBS (phosphate buffer saline), trypsinized for 3 mins with 5 ml of an EDTA/Trypsin solution (0.05 %, 59417C, Gibco, Thermo Fisher), and diluted with low glucose DMEM (Dulbecco's modified Eagle's medium, Sigma-Aldrich, St.Louis, MO, USA) containing 10 % fetal bovine serum (FBS) (# F0244, Sigma-Aldrich, heat-inactivated (30 min, 56°C) and 1 % penicillin-streptomycin (# 17-602E, Lonza, Basel, Switzerland). The cell solution was then centrifuged for 5 min at 1000 rpm, and the resulting pellet was resuspended in 1 ml DMEM. 40,000 cells were plated on ibidi µ-dishes (#81166, ibidi, Germany). 48 hrs post cell seeding in the ibidi dishes, cells were transfected with the 2.5 µg of lifeact-RFP-HaloTag® plasmid using lipofectamine 3000 reagent (L3000001, Thermo Fisher Scientific, Germany). After $\sim$ 48 h expression, small volumes of a 50 nM DNA sensor solution in Phenol red free medium (DMEM,Gibco, 1X, 11880-028, Life Technologies, UK), with 10 % fetal bovine serum (FBS), heat-inactivated (30 min, 56°C),(# F0244, Sigma-Aldrich) and 1 % penicillin-streptomycin (# 17-602E, Lonza, Basel, Switzerland)) was microinjected into the cells using a Transjector 5246 (Eppendorf, Hamburg, Ger, 5246 01084) in combination with Femtotips (Eppendorf, Hamburg, Ger, 930000035). Injection was performed close to the nucleus in 3 s pulses. Lifetime measurements were performed within 1 hour after microinjection of the sensor construct into HeLa cells. FLIM measurements were performed on single cells using a UPLSAPO 100x oil objective with 1.4 NA and scans were recorded from multiple regions of interest. TCSPC histograms of each pixel were computed and then fitted using a bi-exponential decay function. An average

lifetime value was calculated for each pixel, weighing the lifetime components with their respective fluorescence photons (as used for TCSPC fitting). The obtained values of intensity-weighted average lifetimes are color-coded in the FLIM images in Figure S8. Additional confocal micrographs and FLIM images are also shown in Figure S9. Since fluorescence lifetimes are on the order of nanoseconds, they are well separated from the unbinding time ($k_{off}^{-1} = 0.4$ s). Each excitation laser pulse will thus sample the instantaneous fraction of opened and closed sensors. Building up enough photon statistics to evaluate the lifetimes typically takes longer than the sensor bound time, but if the rate of change of stresses in a certain region of the cell is not changing much during the data collection time, the results will still faithfully reflect the average fraction of open vs. closed sensors.

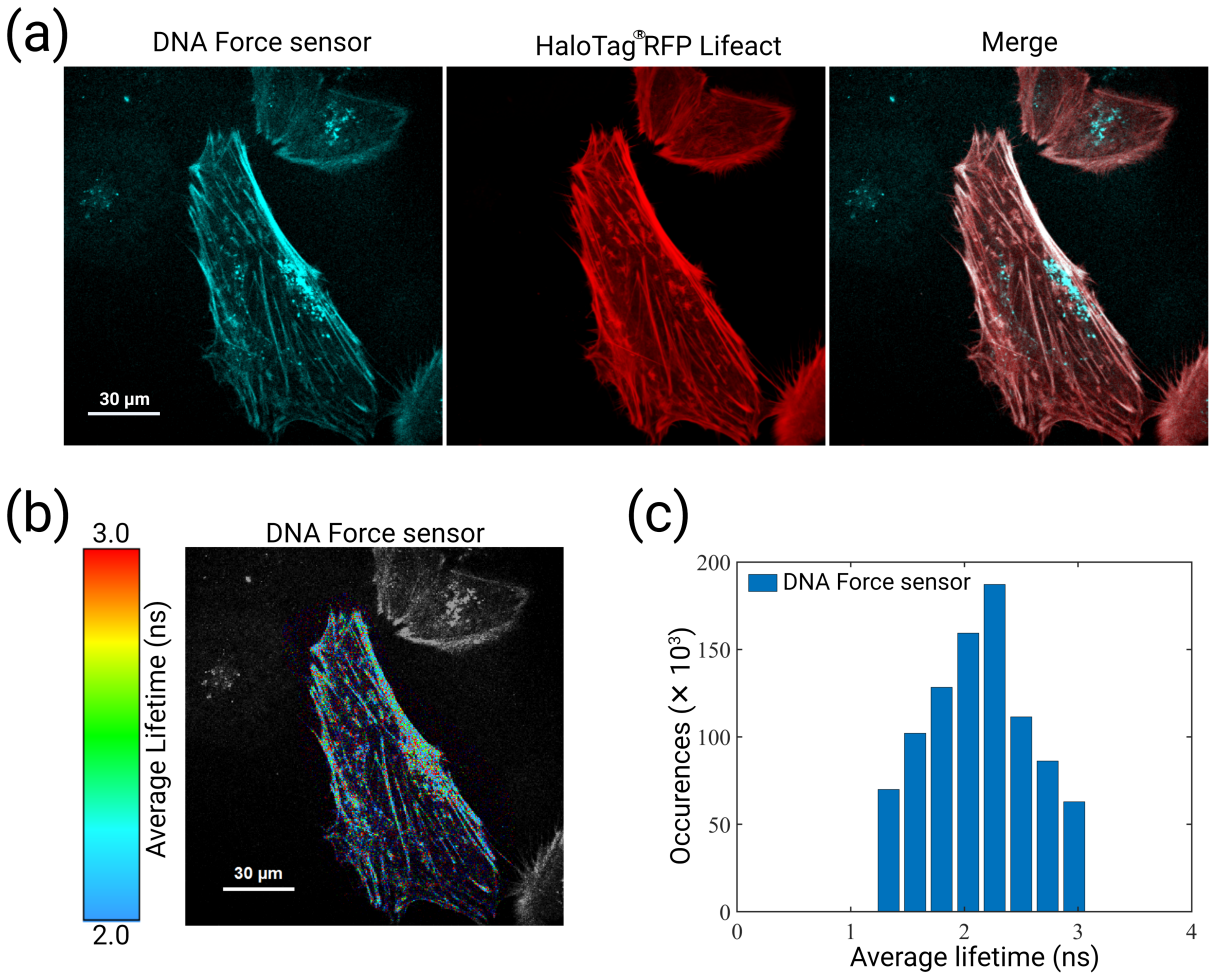

Figure S8: HeLa cells microinjected with closed DNA sensors. **(a)** Confocal micrographs of a cell false-colored for fluorescence intensity. Images corresponding to Alexa 488-tagged closed DNA sensor recorded in the DNA force sensor spectral channel (left), the same cell in RFP spectral channel (middle) and the overlay between both channels (right) confirms co-localization between DNA sensors and actin. **(b)** FLIM image of the same cell as in **(a)** is illustrated for the DNA force sensor spectral channel. **(c)** Bar histogram showing fitted fluorescence lifetimes obtained from **(b)**. An average fluorescence lifetime of 2.2 $\pm$ 0.5 ns was calculated for DNA force sensors.

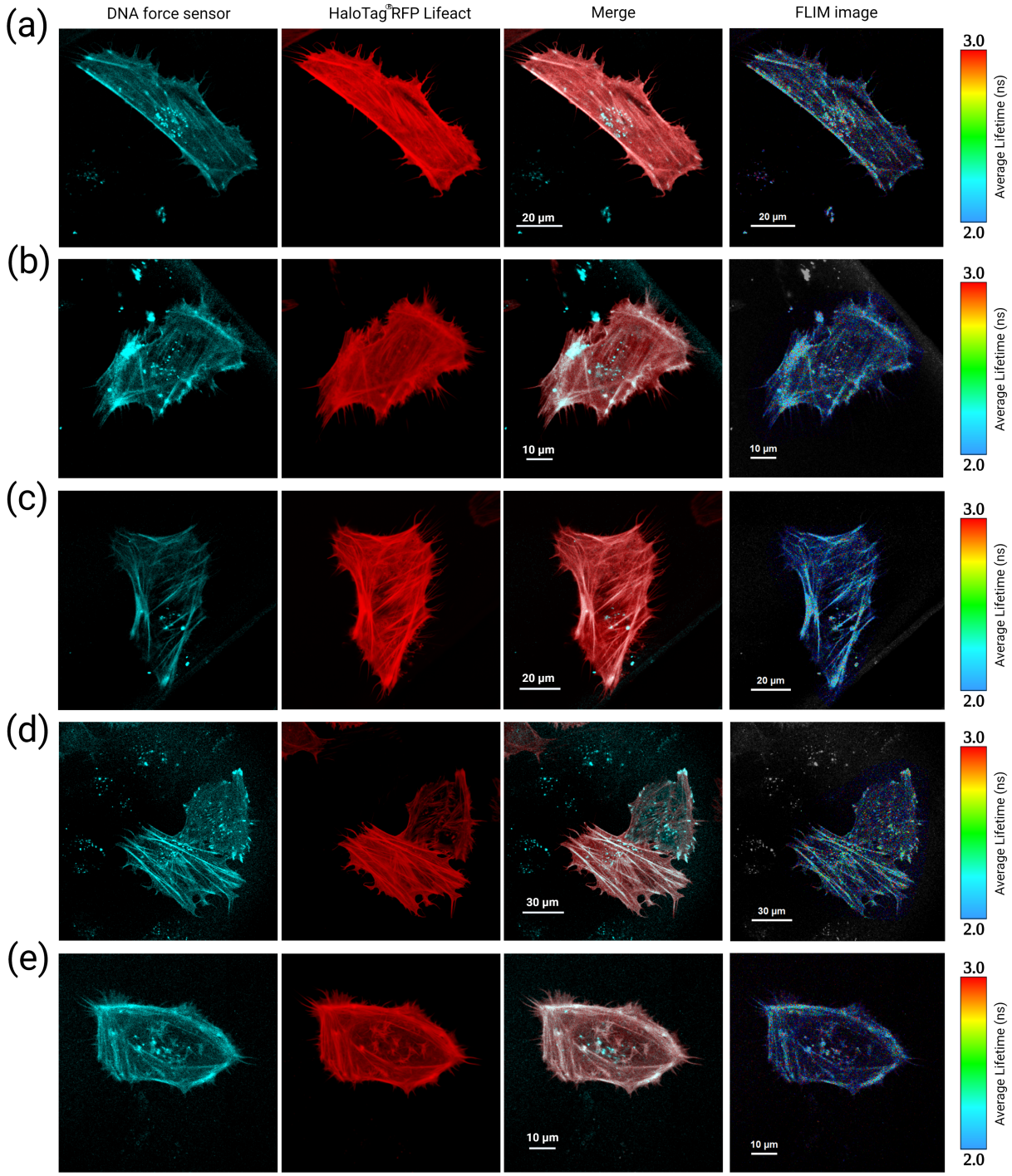

Figure S9: **(a)-(e)** HeLa cells microinjected with closed DNA sensors. From the left: panels show the DNA sensor channel, the RFP channel, the overlay, and FLIM images respectively.

References

(1) Zhang, Y.; Ge, C.; Zhu, C.; Salaita, K. DNA-based digital tension probes reveal integrin forces during early cell adhesion. *Nat. Commun.* **2014**, *5*, 1–10.

(2) Woodside, M. T.; Behnke-Parks, W. M.; Larizadeh, K.; Travers, K.; Herschlag, D.; Block, S. M. Nanomechanical measurements of the sequence-dependent folding landscapes of single nucleic acid hairpins. *Proc. Nat. Acad. Sci. USA* **2006**, *103*, 6190–6195.

(3) Bosco, A.; Camunas-Soler, J.; Ritort, F. Elastic properties and secondary structure formation of single-stranded DNA at monovalent and divalent salt conditions. *Nucleic acids research* **2014**, *42*, 2064–2074.

(4) Odijk, T. Polyelectrolytes near the rod limit. *Journal of Polymer Science: Polymer Physics Edition* **1977**, *15*, 477–483.

(5) Skolnick, J.; Fixman, M. Electrostatic persistence length of a wormlike polyelectrolyte. *Macromolecules* **1977**, *10*, 944–948.

(6) Manning, G. S. Counterion condensation on a helical charge lattice. *Macromolecules* **2001**, *34*, 4650–4655.

(7) Caliskan, G.; Hyeon, C.; Perez-Salas, U.; Briber, R.; Woodson, S.; Thirumalai, D. Persistence length changes dramatically as RNA folds. *Physical review letters* **2005**, *95*, 268303.

(8) Toan, N. M.; Thirumalai, D. Theory of biopolymer stretching at high forces. *Macromolecules* **2010**, *43*, 4394–4400.

(9) Maeshima, K.; Matsuda, T.; Shindo, Y.; Imamura, H.; Tamura, S.; Imai, R.; Kawakami, S.; Nagashima, R.; Soga, T.; Noji, H., et al. A transient rise in free Mg2+

ions released from ATP-Mg hydrolysis contributes to mitotic chromosome condensation. *Current Biology* **2018**, *28*, 444–451.

(10) Romani, A. M. P. In *Magnesium in the Central Nervous System*; Vink, R., Nechifor, M., Eds.; University of Adelaide Press: Adelaide (AU), 2011; Chapter 2, pp 13–58.